

<b>FCH JU Grant Agreement no.:</b>	<b>245113</b>
<b>Project acronym:</b>	KEEPEMALIVE
<b>Project title:</b>	Knowledge to Enhance the Endurance of PEM fuel cells by Accelerated Lifetime Verification Experiments
<b>Funding scheme:</b>	Collaborative Project
<b>Area:</b>	SP1-JTI-FCH.3 Stationary Power Generation & CHP
<b>Start date of project:</b>	01.01.2010
<b>Duration:</b>	36 months
<b>Project Coordinator:</b>	Energy research Centre of the Netherlands ECN (NL)

## Deliverable Report:

### OVERVIEW OF REAL-LIFE OPERATION CONDITIONS

#### (D 1.1)

<b>Author (partner):</b>	Laila Grahl-Madsen (IRD)
<b>Other authors:</b>	Rasmus Munksgaard Nielsen (IRD) Jens Jakobsen (SEAS-NVE) Mathieu Marrony (EIFER)
<b>Workpackage:</b>	WP1, From real-life operation to experimental programme
<b>Workpackage leader (partner):</b>	Laila Grahl-Madsen (IRD)
<b>Date released by WP leader:</b>	27 April 2010
<b>Date released by Coordinator:</b>	04 June 2010

Dissemination level		
PU	Public	X
PP	Restricted to other programme participants (including the Commission Services)	
RE	Restricted to a group specified by the consortium (including the Commission Services)	
CO	Confidential, only for members of the consortium (including the Commission Services)	

Revisions			
Version:	Date:	Changed by:	Comments:
1.00	27 April 2010	Laila Grahl-Madsen	
1.01	10 May 2010	Laila Grahl-Madsen	Minor corrections
1.10	11 May 2010	Laila Grahl-Madsen	Changes made on base of input from M. Marrony
1.11	17 May 2010	Laila Grahl-Madsen	Start-up/shutdown section revised
1.12	04 June 2010	Laila Grahl-Madsen	Reformat composition corrected p.17
1.13	10 June 2010	Laila Grahl-Madsen	$P_{TH}$ nominal value corrected for the $\gamma$ - $\mu$ CHP in Fig. 3.

## TABLE OF CONTENT

---

<b>1 The Hydrogen fuelled LT PEM <math>\mu</math>CHP.....</b>	<b>3</b>
1.1 Introduction to the Danish $\mu$ CHP demonstration project.....	3
1.2 The LT PEM $\mu$ CHP.....	5
1.2.1 The state-of-the-art IRD LT PEM MEA and Stack Technology .....	5
1.2.2 The Hydrogen Circuit.....	8
1.2.3 The Air Circuit .....	8
1.2.4 The Thermal Circuit .....	9
1.2.5 The Electrical Circuit .....	9
1.2.6 Nominal Operation .....	9
1.3 Operational Experience .....	10
1.3.1 Operational Patterns based on Heat demand.....	10
1.3.2 VPP Operational Patterns .....	10
1.3.3 Operational Field Test Experience with the $\beta$ - $\mu$ CHP .....	11
1.3.3.1 Hot Spots .....	12
1.3.3.2 Start-up and shutdown.....	13
<b>2 The Reformat Fuelled LT PEM <math>\mu</math>CHP .....</b>	<b>14</b>
2.1 Introduction .....	14
2.2 Field test of PEM FC from Vaillant Technologies.....	14
2.2.1 System description .....	14
2.2.1.1 The Valliant LT PEM.....	16
2.2.1.2 Fuel Processor .....	17
2.2.1.3 Other operational parameters .....	18
2.2.1.4 Start-up .....	19
2.2.2 Performance.....	19
2.2.3 Reliability of the system.....	21
2.3 LT PEM FC MEA Operation with Simulated Reformat.....	24
<b>3 Conclusion and Recommendations.....</b>	<b>26</b>
<b>4 References .....</b>	<b>27</b>
<b>Annex 1. Abbreviations.....</b>	<b>28</b>

## 1 THE HYDROGEN FUELLED LT PEM $\mu$ CHP

### 1.1 INTRODUCTION TO THE DANISH $\mu$ CHP DEMONSTRATION PROJECT

The Danish  $\mu$ CHP (micro combined heat and power<sup>1</sup>) project<sup>2 & 3</sup> develops and tests fuel cells integrated into units aimed for single family houses.  $\mu$ CHPs based on three different types of fuel cells (LT PEM, HT PEM & SOFC) is developed within the Danish project. The LT PEM units are solely developed by IRD, and aimed for pure hydrogen fuelling. The project status is as follows (Mar-2010):

- Phase 1 is completed. The phase comprises construction and test of three prototype ( $\alpha$ -)  $\mu$ CHPs each based on one of the FC-technologies (Fig. 1)
- The LT PEM based  $\mu$ CHP technology has been completed for phase 2 also. Five (5)  $\beta$ - $\mu$ CHP units were in phase 2 installed in ordinary single family houses (Fig. 2) in the village Vestenskov, situated at the Danish island Lolland
- The SOFC and the HT PEM  $\mu$ CHP technologies are in the middle of phase 2. None of these technologies have been CE-certificated nor installed for field test yet
- The LT PEM  $\mu$ CHP field test comprises 35 units, and is scheduled to begin in Q2-2010. The  $\gamma$ - $\mu$ CHP has been constructed and CE-certified (Fig. 3)

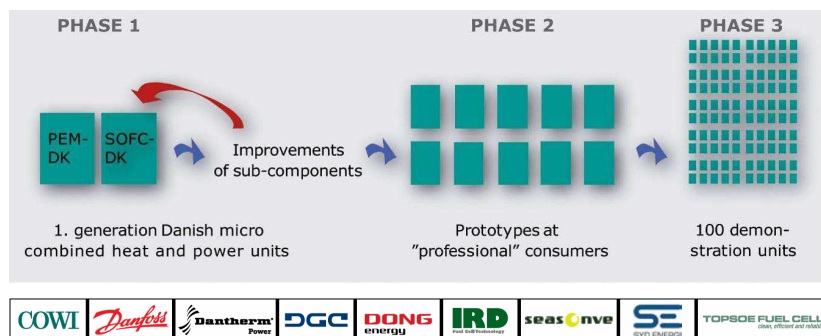


Fig. 1 The three project phases of the Danish  $\mu$ CHP project, and the project participants. The project coordination has recently been taken over by SEAS-NVE, as Danfoss (prior coordinator) withdrew from the project.

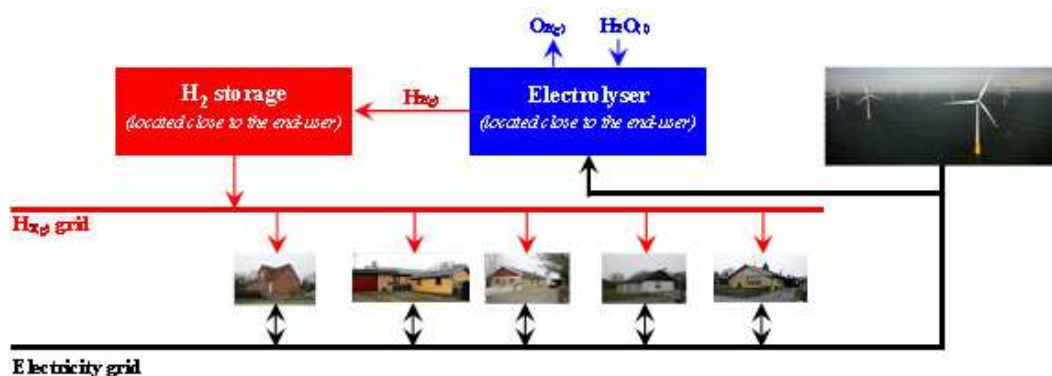


Fig. 2 The Danish concept on storing surplus energy (wind) by water electrolysis, for later use by the  $\mu$ CHPs.

<sup>1</sup> Abbreviations are listed in Annex 1

<sup>2</sup> Partly funded by Energinet.dk (phase 1) and The Danish Energy Agency (phase 2 & 3) through the contracts: PSO J.no. 2006-1-6295, and EFP-Akt.167 J.no. 033001/33033-0151, respectively

<sup>3</sup> Further information can be found at <http://www.dk-mchp.eu/project.html>



2006/7 The IRD  $\alpha$ - $\mu$ CHP unit has the following key characteristics:

Nominal power:	1.5 kW <sub>AC</sub>
Power range:	0.9-2.0 kW <sub>AC</sub>
Nominal heat:	1.1 kW <sub>TH</sub>
Heat Range:	0.5-1.1 kW <sub>TH</sub>
Efficiency (LHV) at nominal operation:	
Electrical (H <sub>2</sub> →P <sub>DC</sub> )	49%
Electrical (H <sub>2</sub> →P <sub>AC</sub> )	43%
Combined efficiency	75%
Stand-by-power:	85 W <sub>AC</sub>
Ready-mode Power:	105 W <sub>AC</sub>



2008/9 The IRD  $\beta$ - $\mu$ CHP unit has the following key characteristics:

Nominal power:	1.5 kW <sub>AC</sub>
Power range:	0.9-2.0 kW <sub>AC</sub>
Nominal heat:	1.5 kW <sub>TH</sub>
Heat Range:	0.8-2.0 kW <sub>TH</sub>
Efficiency (LHV) at nominal operation:	
Electrical (H <sub>2</sub> →P <sub>DC</sub> )	52%
Electrical (H <sub>2</sub> →P <sub>AC</sub> )	47%
Combined efficiency	94%
Ready-mode Power:	40 W <sub>AC</sub>



2009/10 The IRD  $\gamma$ - $\mu$ CHP unit has the following key characteristics:

Nominal power:	1.5 kW <sub>AC</sub>
Power range:	0.9-2.0 kW <sub>AC</sub>
Nominal heat:	1.6 kW <sub>TH</sub>
Heat Range:	0.5-2.0 kW <sub>TH</sub>
Efficiency (LHV) at nominal operation:	
Electrical (H <sub>2</sub> →P <sub>DC</sub> )	47%
Electrical (H <sub>2</sub> →P <sub>AC</sub> )	44%
Combined efficiency	94%
Ready-mode Power:	15 W <sub>AC</sub>

Fig. 3 Key numbers and pictures (almost the same scale) of IRDs hydrogen fuelled  $\mu$ CHP based on the LT PEM technology.



Key numbers electrolyser:

- Gas Outlet Pressure up to a 8 bar(g)
- Max Hydrogen production 20 Nm<sup>3</sup>/h
- Max Oxygen production 10 Nm<sup>3</sup>/h
- Continuously H<sub>2</sub> production 16 Nm<sup>3</sup>/h
- Continuously O<sub>2</sub> production 8 Nm<sup>3</sup>/h
- Gas Purity 99.5 ± 0,1%
- Max electric energy consumption 104 kW

Key numbers H<sub>2</sub>-storage:

- 25 Nm<sup>3</sup>
- 0-6 bar(g)

Fig. 4 Picture and key-numbers of the alkaline electrolyser installed in Vestenskov (project phase 2).

The main difference between the  $\alpha$ - and the  $\beta$ - $\mu$ CHP is related to efficiency (Fig. 3), while the main difference between the  $\beta$ - and the  $\gamma$ - $\mu$ CHP is related to cost (reduced with more than 60%), size, and easier to service and repair.

The  $\mu$ CHP is connected to a 200 litre heat storage tank.

An electrolyser has been installed centrally in Vestenskov for fuelling the five  $\mu$ CHPs in the project phase 2 (Fig. 4). A hydrogen distribution grid has been buried.

The initiation of the phase 2 field test was delayed almost 9-month due to lack of authority approval of the hydrogen pipe that enters the house (c. 10- 30 cm of piping). The phase 2 was finally initiated, but only with a dispensation not a final approval.

The five (5) phase 2  $\beta$ - $\mu$ CHP units has been in field test for a period compromised the (summer)autumn-winter 2009. The phase 2 is now completed for the LT PEM technology.

## 1.2 THE LT PEM $\mu$ CHP

### 1.2.1 THE STATE-OF-THE-ART IRD LT PEM MEA AND STACK TECHNOLOGY

The state-of-the-art LT PEM MEA is based on Nafion NR212<sup>4</sup>, Cabot carbon supported catalyst<sup>5</sup>, and SGL DC30 GDL (Freudenberg GDL is under implementation). The present state-of-the-art MEA is not reinforced, but reinforcement is being implemented in the production shortly. Several reinforcement foils are presently being examined. It is important that the reinforcement rim protects the membrane from the 'needles' at the GDL edge that often puncture the membrane.

<sup>4</sup> [http://www2.dupont.com/FuelCells/en\\_US/assets/downloads/dfc201.pdf](http://www2.dupont.com/FuelCells/en_US/assets/downloads/dfc201.pdf)

<sup>5</sup> Anode loading: 0.3 mg PtRu per cm<sup>2</sup> and cathode loading 0.5 mg Pt per cm<sup>2</sup>



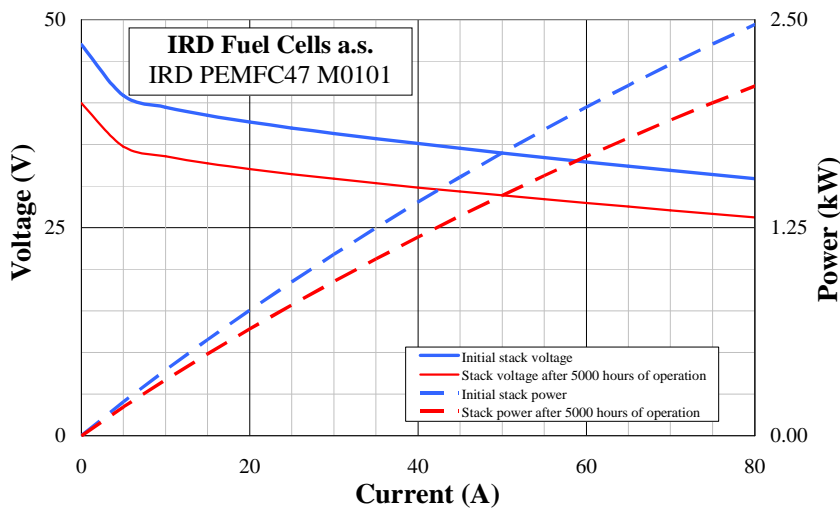


Fig. 5

Stack performance at BoL and as calculated after 5,000 hours of operation<sup>6</sup>.

Table 1 Nominal operation parameters.

$\beta$ - $\mu$ CHP:	Operated on base of heat demand (cf. section 1.3.1)
$\gamma$ - $\mu$ CHP:	Operated as a simulated VPP (cf. section 1.3.2)
Fuel:	“Pure hydrogen” (alkaline electrolyser)
	Dew point: $-20^{\circ}\text{C}$
	Pressure: $\approx 400$ mbar
	Lambda: $\approx 1.01$
Oxidant:	’Fresh’ air from outdoor
	Dew Point: $\approx 57^{\circ}\text{C}$
	Lambda: $\approx 2.7$
Nominal load:	$0.35 \text{ A/cm}^2$
Temperature:	$T_{\text{In}} 62^{\circ}\text{C}$
	$T_{\text{Out}} 65^{\circ}\text{C}$

The state-of-the-art IRD MEA is fabricated by ultra sonic spray coating GDL (CCB). However, MEAs fabricated by catalyst coating the membrane (CCM) is presently under implementation as standard.

The IRD  $\mu$ CHPs are in all versions equipped with a 47-cell stack with a performance as shown in Fig. 5. The bipolar plates are made by graphite composite material aimed for long lifetime. The bipolar plates are moulded in-shape at IRD by compression moulding. A serpentine flow field is applied on both the anode and the cathode. The active electrode area is  $156.25 \text{ cm}^2$ . The number of cells in the stack has been selected as a trade off between stack cost and performance, taking into account that the FC-power @ BoL needs to be above 1.7 kW and simultaneously operate with a

<sup>6</sup> Assuming a degradation rate of  $10 \mu\text{V/h}$  (c.f. Fig. 30) including many start/stops, as described in later sections

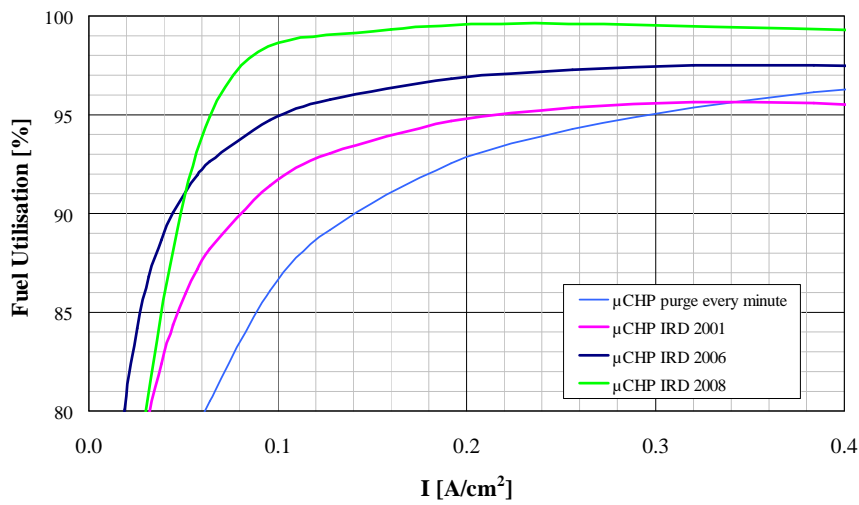


Fig. 6

Fuel [H<sub>2</sub>] utilisation in the  $\beta$ - $\mu$ CHP (equivalent to utilisation in the  $\gamma$ - $\mu$ CHP).

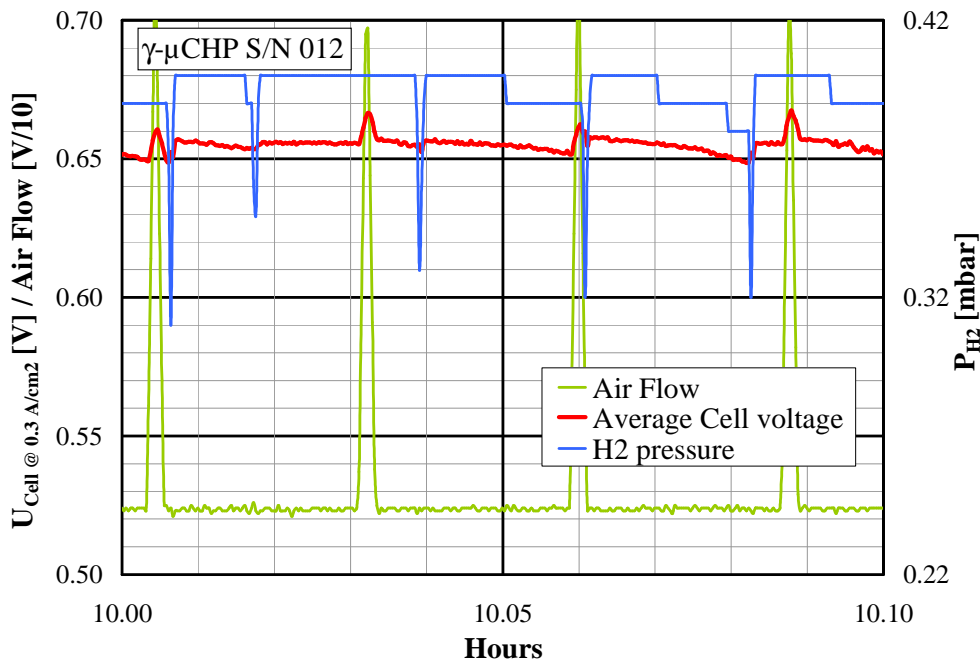


Fig. 7

Cell voltage at nominal load upon hydrogen purge and air 'purge' in the  $\gamma$ - $\mu$ CHP.

Table 2 Summary of gas and fluid configuration in the  $\beta$ - and the  $\gamma$ - $\mu$ CHP stack.

Fluid	Flow pattern	Stack orientation
Air	U	Vertical
Fuel	Z	
Cooling water	Z	

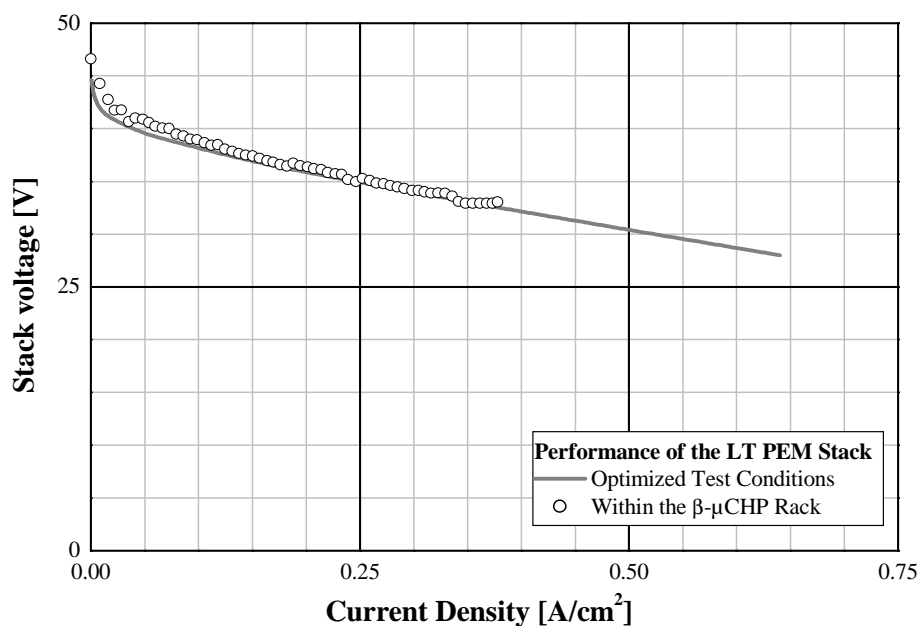


Fig. 8

Stack performance in open-end R&D tests (cf. Fig. 5) compared with the stack performance in the dead-end β-μCHP system.

maximum current of 60 A into the inverter. The nominal operational conditions of the LT PEM FC stack are listed in Table 1. The standard stack connections are listed in Table 2.

All IRDs LT PEM stacks are equipped with in-house designed and constructed cell voltage monitoring system (CVMS) having a resolution of  $\pm 20$  mV. The CVMS has proven to be very important in the BoP-control cf. section 1.3.3.

### 1.2.2 THE HYDROGEN CIRCUIT

The μCHP is operated with 'pure' hydrogen after the dead-end principle where the hydrogen circuit is closed with a solenoid valve at the outlet. The dead-end operation is applied to enhance the fuel utilisation (Fig. 6) and the overall system efficiency. The solenoid valve is opened approximately 1 s every minute to remove accumulated water on the anode electrode (purge), Fig. 7. The hydrogen loss during purge depends on the stack and system.  $\approx 1$  litre of hydrogen is ventilated during purge in the IRD μCHP. However, the system is designed not to ventilate more than four (4) litre of hydrogen to the ambient per hour; the other purges are made internally in the system. The hydrogen supply is  $\approx 400$  mbar to ensure a sufficient flow even within the purge situations. The supply hydrogen has a low dew point (c.  $-20^\circ\text{C}$ ).

### 1.2.3 THE AIR CIRCUIT

The cathode pressure is ambient, and the air is supplied by a blower. The oxygen stoichiometry is at nominal conditions 2.7. However, the air supply is increased briefly (once every 100 s) to remove accumulated water on the cathode. This pattern has been applied to ensure the lowest possible power consumption of the air blower, while simultaneously avoid water management problems.

The air is humidified by a passive membrane humidifier that utilise the humid cathode exhaust to heat and humidify the FC air supply. The approach temperature obtained is  $8^\circ\text{C}$ .

The air intake is realised by a balanced ventilation of the μCHP cabinet. The μCHP air intake is equipped with a filter active for organic components; the air filter fulfils the DIN 71460 efficiency standard.



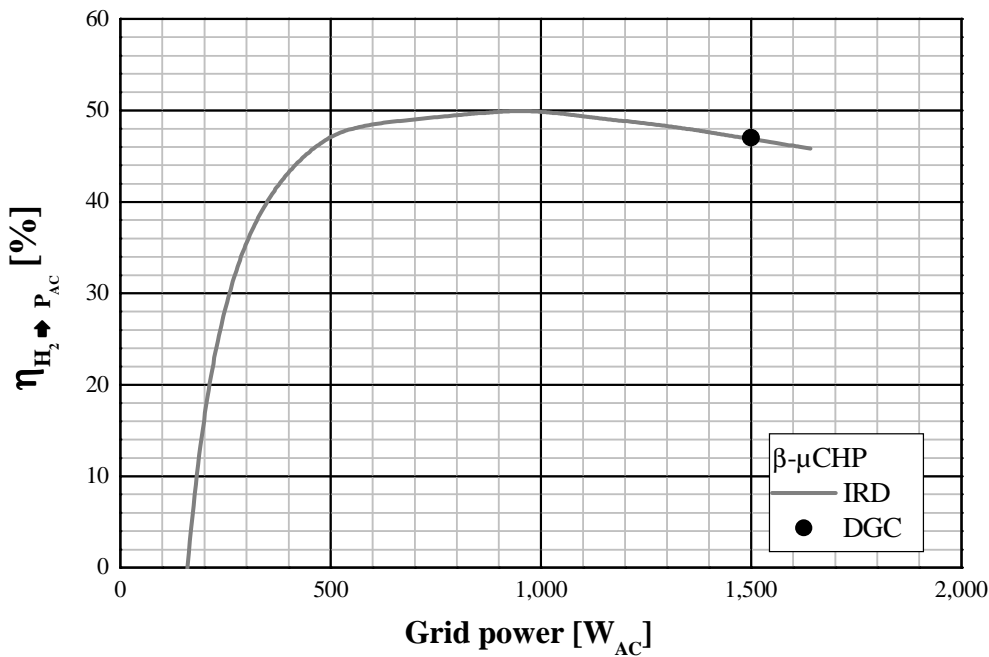


Fig. 9  
AC-power efficiency of the  $\beta$ - $\mu$ CHP. DGC is an independent Danish Gas Technological Centre.

### 1.2.4 THE THERMAL CIRCUIT

The 47-cell IRD stack is liquid cooled with DI water at present. The  $\mu$ CHP primary cooling circuit is connected to the secondary cooling circuit (the central house heating) through a heat-exchanger. The primary cooling circuit is equipped with an open expansion tank.

### 1.2.5 THE ELECTRICAL CIRCUIT

The  $\mu$ CHPs are all electrically connected to the 230 V<sub>AC</sub>-grid through an inverter (commercial available inverter). The present inverter efficiency is rather low (92%).

The 24 V power for the BoP components are delivered directly from the 230 V<sub>AC</sub>-grid, and not yet through the inverter.

### 1.2.6 NOMINAL OPERATION

An expression of the capability of the system to ‘nurse’ the stack can be found in Fig. 8, where the polarization curve obtained in a R&D test stand with optimal operational conditions is compared with the polarization curve obtained in the  $\beta$ - $\mu$ CHP. The two curves show insignificant deviations, leading to the conclusion that the short term operational conditions in the  $\mu$ CHP are acceptable.

The system efficiency measured at IRD and at The Danish Gas Technology Centre (DGC) is shown in Fig. 9. The  $\beta$ - $\mu$ CHP efficiency does not peak at nominal power (1.5 kW<sub>AC</sub>). The efficiency number listed for the  $\gamma$ - $\mu$ CHP in Fig. 3 are slightly lower than for the  $\beta$ - $\mu$ CHP. This is due to the following two factors:

- The substantial cost reduction obtained between the  $\beta$ - and the  $\gamma$ - $\mu$ CHP unit has resulted in choosing a few much cheaper, but less efficient BoP components
- The efficiency of the  $\beta$ - $\mu$ CHP was measured on a ‘fresh’ almost unused-unit, while the efficiency of the  $\gamma$ - $\mu$ CHP was measured on a unit that had been in operation for 1,000 h’s

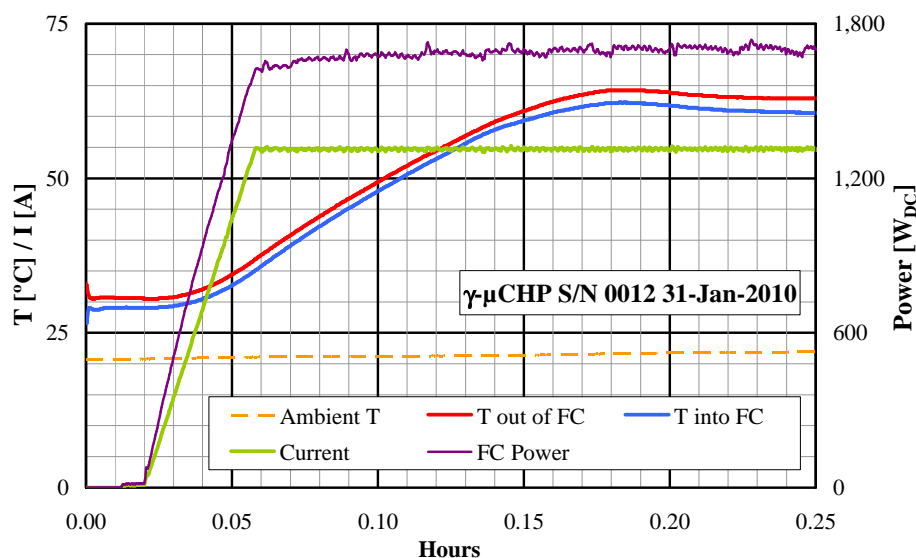


Fig. 10  
Temperature, current and FC power during a cold start-up.

A typical load profile during cold start of the  $\beta$ - and  $\gamma$ - $\mu$ CHP is shown in Fig. 10. The load increase rate is 0.3 A/s (if the min. cell voltage is above 0.4 V), which means full load within 3 minutes. The operational temperature is then reached within  $\approx 10$  min.s, depending on the ambient temperature.

The  $\mu$ CHPs ( $\beta$ - &  $\gamma$ -version) are solely remote operated through an Ethernet connection. The data-logging frequency is every 60 seconds. The last operational hour is logged every second. This log-file can be downloaded for data-processing, but data older than one hour are deleted as it is a running log. The log-files contain all set-points, actual measurements of temperature, stack & inverter current and voltages as well as all individual cell-voltages.

### 1.3 OPERATIONAL EXPERIENCE

#### 1.3.1 OPERATIONAL PATTERNS BASED ON HEAT DEMAND

The  $\beta$ - $\mu$ CHP unit has been operated on base of the heat demand. This causes limited operation during summer with many start-stops (Fig. 11) varied with the number and age of the occupants (1-3 grown-ups with 0-2 children). However, the heat demand in Denmark during winter and in particular the demand during the cold winter 2009/10 made most of the  $\mu$ CHPs runs continuously. The existing oil-fired boilers having not been removed from the test houses during the phase 2 field test (of the  $\beta$ - $\mu$ CHPs).

All five (5) field  $\beta$ -test units have, in general been exposed to very different consumption pattern.

#### 1.3.2 VPP OPERATIONAL PATTERNS

The  $\gamma$ - $\mu$ CHP field test will be done differently than the phase 2 field test. The  $\mu$ CHP will within this field test act as virtual power plants (VPPs)<sup>7</sup>, which mean that they will be operated as grid equalisation units upon high power demand and/or on high power spot price. It is not yet possible to

<sup>7</sup> The VPP-vision is very important in Denmark due to the high amount of wind-power installed.

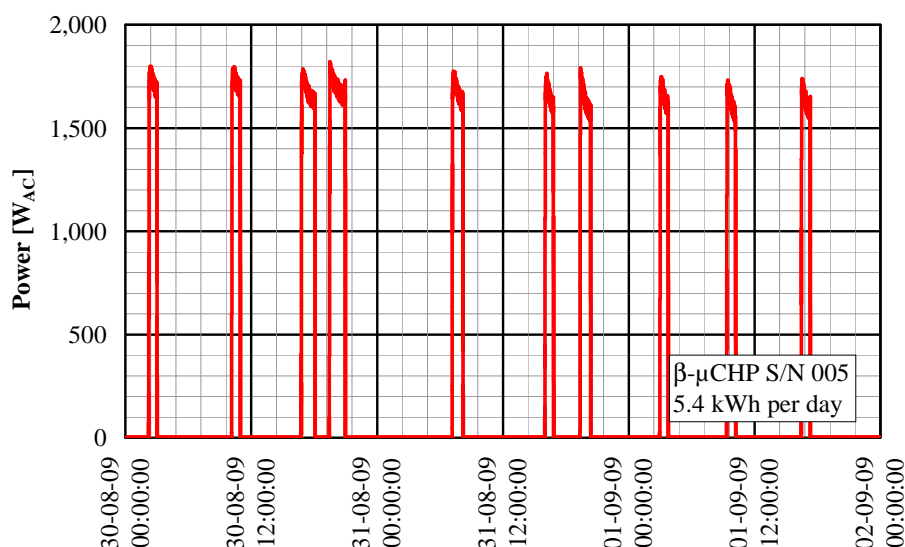


Fig. 11

Summer operation based on heat demand.

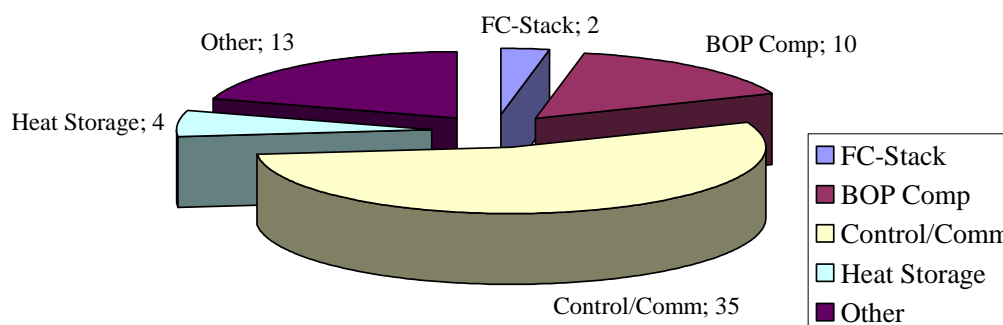


Fig. 12 Recorded types of failures during the field test of the β-μCHP units in Vestenskov.

make a full VPP-test. It has therefore been decided to make a simulated VPP-test. The test year has preliminary been divided into a summer and a winter period. The operational patterns in the two periods will be as follows:

- Winter: Eight operational hours a day divided into the following two time spans: 7 AM -11 AM and 4 PM – 8 PM. This will result in a production of 12 kWh<sub>AC</sub> and 12 kWh<sub>TH</sub>. The heating storage is equipped with 12 kW electrical heating elements, which will be activated in case the heat produced by the μCHP doesn't cover the heat demand.
- Summer: Max. six hours a day within the time span 8 AM -2 PM. An average 'heat' demand to utility water for a single family within Denmark during the summer is 7 kWh<sub>TH</sub>.

### 1.3.3 OPERATIONAL FIELD TEST EXPERIENCE WITH THE β-μCHP

There have been many lessons learned in the phase 2 field test. An overview of the recorded failures from the field test of the five β-units in Vestenskov are summarised in Fig. 12. However, it is important to bear in mind that almost all failures outside the PEM stack results in unfavourable LT PEM MEA conditions leading to reduced durability/lifetime e.g. drying out, H<sub>2</sub>/O<sub>2</sub> starvation, carbon corrosion. It is therefore important to consider the BoP in order to enhance the lifetime, but this subject is outside the scope of the present project. However, an important expected outcome of

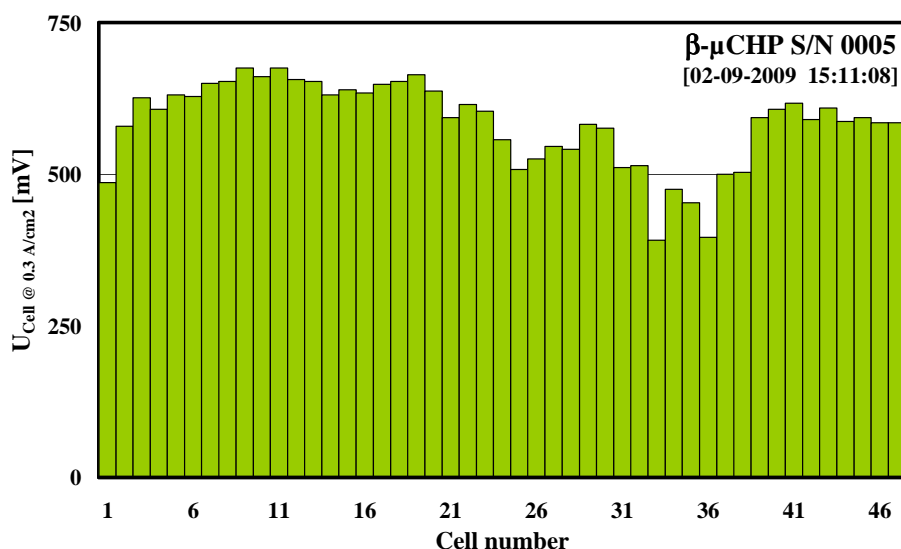


Fig. 13  
V-shaped cell voltage at 55 A.

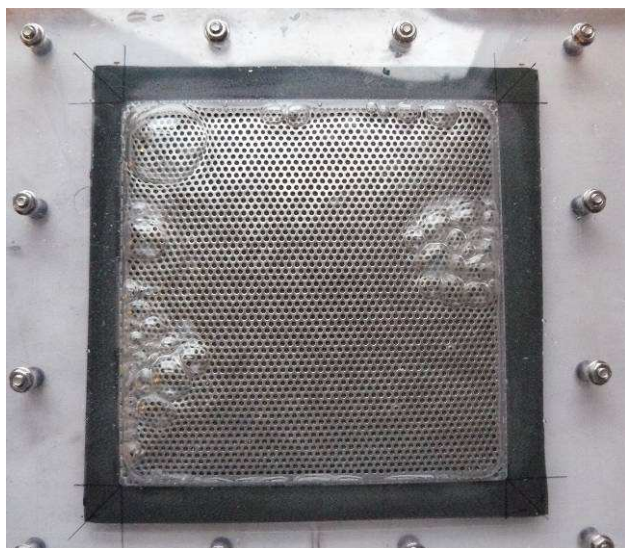


Fig. 14  
Simplified test for visual inspection of pin-hole location in a failed MEA. The MEA is fixed in a frame with a perforated plate on top (c.12.5\*12.5 cm). The MEA is exposed to air underneath and water on top. Air bobbles going through the MEA locate the position of the pin-holes e.g. along the GDL edge at the manifold position.

the KeepPEMALive project is not only improved materials, but also guidelines in optimal operational strategies.

Some failures have been related to control errors of the heat storage, where the heat storage mistakenly has heated up the FC-stack through the heat exchanger. Temperatures in excess of 80°C have occurred for longer time in such situations. This has not caused instant MEA failures, but has contributed to a limited MEA-lifetime.

Below is discussed the most important/relevant other failures observed.

### 1.3.3.1 Hot Spots

Uneven cooling, e.g. due to air trapped in the cooling circuit, results in local overheating of some cells, often several neighbouring cells. A typical picture of the individual cell voltages in such a situation is shown in Fig. 13. The situation can occur at too low cooling water level or just after maintains where fresh cooling water has been added. The local hot spot results in dry MEAs, particularly the membranes dry out and do for this reason become less mechanical stable during the

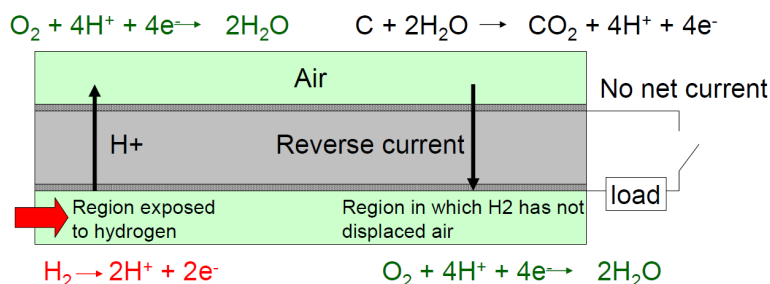


Fig. 15

The unmitigated start/stop mechanism (Motupally 2007).

dead-end operation (pressure pulsing cf. Fig. 7) and cross-over can occur as a consequence of this (Fig. 14).

### 1.3.3.2 Start-up and shutdown

The majority of the failures are, as discussed previously, not related to the FC stack itself, but particularly related to the control and the communication particularly during start-up or at shutdown. Fuel starvation e.g. due to flooding can typically occur during cold start-up resulting in cell reversing and/or destruction, if the unfortunate situation occurs while loaded and the system response is too slow or the cell voltages not is ‘contumeliously’ monitored.

- Cathode flooding: Protons are passed through the membrane to form hydrogen in the absence of oxygen, and the cell essentially acts as a hydrogen pump. The cathode potential drops due to the lack of oxygen and the presence of hydrogen, and the cell voltage drops to very low levels or may even become negative
- Anode flooding: When hydrogen no longer is available to be oxidized, the anode potential will rise to that required to oxidize water, assuming water is available, resulting in the evolution of oxygen and protons at the anode. The protons will pass through the membrane and combine with oxygen at the cathode in the normal reduction reaction to produce water. Anodes based on catalyst supported on carbon are prone to degradation during fuel starvation due to oxidation of carbon, which is catalyzed by the presence of platinum. The catalyst support is converted to CO<sub>2</sub>, and Pt and/or Ru particles may be lost from the electrode, resulting in loss of performance.

The hydrogen pressure is released upon shutdown and the air-fan stopped. Air will then eventually fill the fuel and air manifolds on extended shutdown. Start-up therefore requires displacing air with fuel/hydrogen. The non-homogeneous mixture of H<sub>2</sub> on the anode is the root cause for unmitigated carbon corrosion where the H<sub>2</sub>/Air portion of cell drives “reverse current” elsewhere (on the Air/Air part of the cell), cf. Fig. 15.

## 2 THE REFORMAT FUELLED LT PEM $\mu$ CHP

### 2.1 INTRODUCTION

Ideally a PEM fuel cell needs to be fuelled by clean hydrogen, another possibility is operation using reformat. This is in particular interesting for areas with natural gas implemented. The natural gas is reformed into a mixture of hydrogen and CO<sub>2</sub> with a small fraction of CO. In particular the CO content is very undesirable since it is known to compromise the fuel cell performance. This is often circumvented by a small air bleed which eliminates the CO at the expense of the overall efficiency.

EDF (Electricité de France) via EIFER institute launched in the past (2004-2007) a wide field experimental testing of four (4) Vaillant technology based on LT-PEM FC technology. Three (3) of these units were installed in the heating rooms of social housing in Sarreguemines, Giromagny, and Orléans (Fig. 16). The fourth one was first used to carry out lab tests and afterwards installed in Liévin afterwards. The lab test was carried out at the EIFER fuel cell test laboratory at the University of Karlsruhe. The unit was installed in a test stand, which provides a natural gas supply; a grid feed in point, a deionised water supply, a thermal load bank for simulating heat demands and a ventilation system for the flue gases. The present report relates main results deduced from this study, and especially from Orléans campaign. The exact total operation hours of the field test are not known, but the field test has been in operation for 20 months (>5,000 h for the stack/system).

### 2.2 FIELD TEST OF PEM FC FROM VAILLANT TECHNOLOGIES

#### 2.2.1 SYSTEM DESCRIPTION

The Vaillant heating system is presented in Fig. 17. The system is composed by:

- A fuel cell system
- A pre-storage water tank of 500 litre is used minimize the start and stop events of the fuel cell, which can worsen the degradation.



Fig. 16

Experimental field testing of Vaillant Euro2 technology by EDF-EIFER.



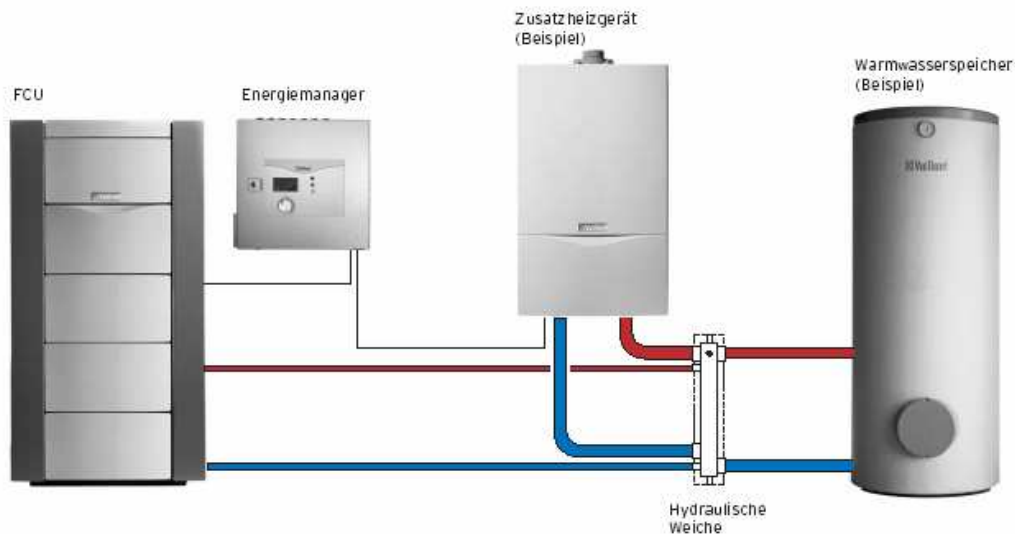


Fig. 17 Description of the boiling system of the PEMFC Vaillant technology setup.

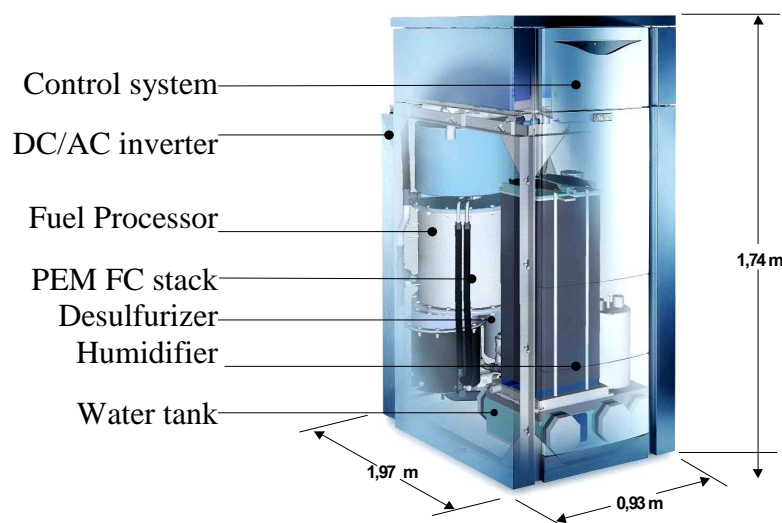


Fig. 18

Overview of the PEM fuel cell system including the natural gas reformer.

An energy manager controls and regulates the fuel cell system online (external temperature measurements, valves opening control, power demand application and definition...). Vaillant specifications require a return temperature of the hot water line below 55°C in order to avoid overheating of the system. According to the thermal demand, the energy manager increases or decreases the electrical power signal (steps of 0.5 kW) between 1.5 to 4.5 kW.

The heating system is furthermore connected with two gas boilers that will help the fuel cell in situations where the heating demand exceeds the production capability. The fuel cell setup including reformer is displayed in Fig. 18. It is seen that the complete system is rather extensive and a reduction of the size would be favourable.

The technical data of the PEM FC is shown in Table 3. Here is seen that the expected lifetime of the stack is 4,000-6,000 hours. And that the electrical output may be altered between 1.5 and 4.6 kW.

Table 3 Overview of the technical specifications of the Vaillant PEMFC system.

Type	EURO2 fuel cell heating appliance
Manufacturer	Vaillant / Plug Power
Electrical power output	1.5 – 4.6 kW
Thermal power output	3.0 – 9.1 kW
Electrical	>30%
Total efficiency	>86%
Maximum number of cold start-ups	<125 per year
Expected stack lifetime	4,000-6,000 hours
Fuel	Natural gas
Supply pressure:	20 mbar
Fuel consumption H (LHV = 9,5 kWh/m <sup>3</sup> )	1.8 m <sup>3</sup> /h
Fuel consumption L (LHV = 8,1 kWh/m <sup>3</sup> )	2.1 m <sup>3</sup> /h
Primary cycle max. pressure	3 bar
Max. flow temperature ( <b>Operating temperature</b> )	70°C
Max. return temperature	55°C
Primary cycle flow rate	~ 1,000 l/h
NO <sub>x</sub> emissions	minimal
CO emissions	<20 ppm
Protection degree	IP 20
Starting time	60 – 150 min

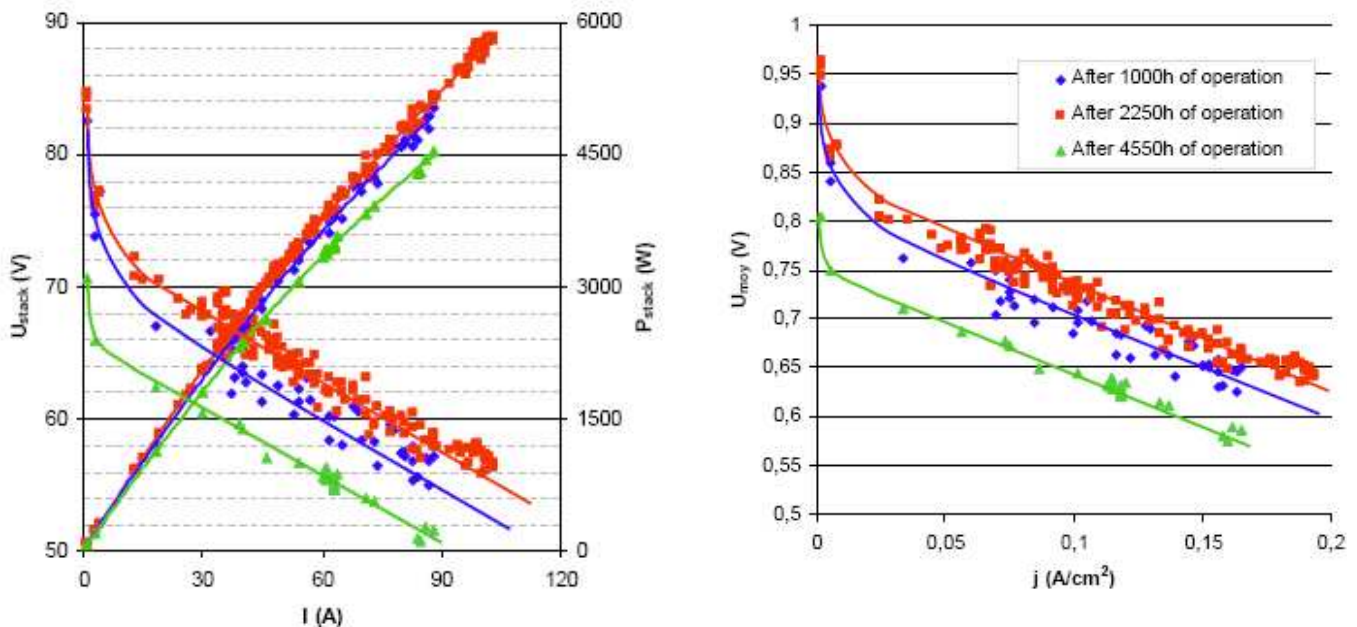


Fig. 19 Polarization curve (reconstructed) of stack vs. time.

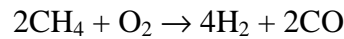
### 2.2.1.1 The Vaillant LT PEM

A remarkable ageing impacting the catalytic activity of stack is noticed with time (strong voltage decrease at low currents) but didn't impact cell resistance (parallel curves at higher current) which reveal a good water management of the system (Fig. 19).

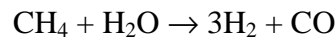
## 2.2.1.2 Fuel Processor

Natural gas is firstly desulfurized and deodorized in order to avoid any stack degradation, then saturated by water in a humidifier. The gas is then decomposed into hydrogen in 3 following steps:

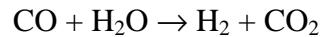
- An autothermal reaction (ATR): the natural gas is decomposed into CO and H<sub>2</sub>, in the range of operation of temperature between 550 and 920°C, by following two simultaneous chemical reactions:



And



- The oxidant reaction of CO or "Low temperature gas shift" (LTS) made in range of temperature 200-220°C, within the following reaction:



- The preferential oxidant reaction which oxidize the residual CO (between 2,000 and 3,000 ppm) into CO<sub>2</sub> in order to reduce the final concentration of CO to less than 50 ppm. The reaction is operated between 120 and 150°C.

The excess of H<sub>2</sub> not consumed by the stack is burnt in the temperature range 500-800°C during the oxidant reaction of outlet anode gas ("anode gas tail oxidiser", ATO).

This free energy is used to heat up and regulate the temperature of humidifier which will saturate the air/natural mix gas into pure water dedicated to ATR (drying effect avoided for the system). The water of the flow circuit of stack is used to heat up the pre-storage tank. The final reformat typically had the following composition: 73% H<sub>2</sub>, 19% CO<sub>2</sub>, 8% N<sub>2</sub> and <20 ppm CO.

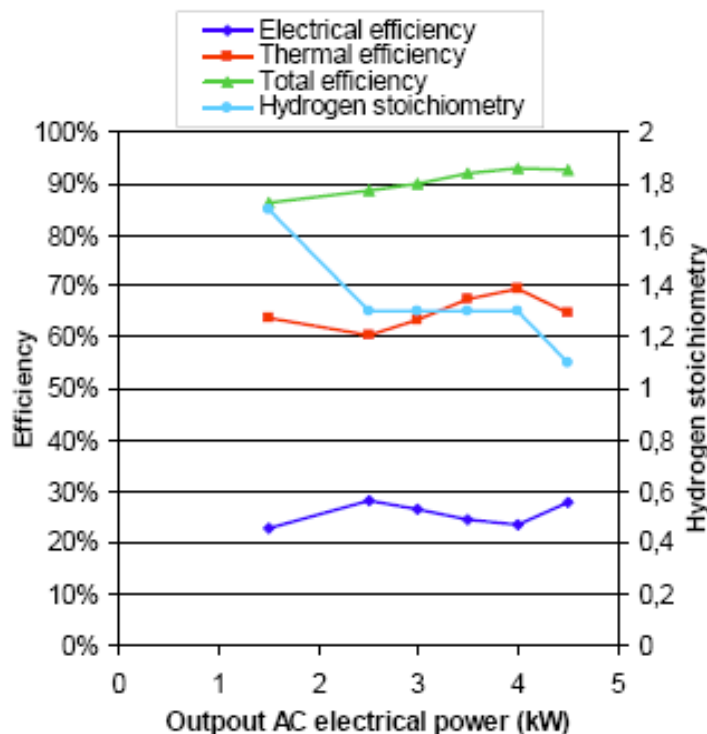


Fig. 20

Evolution of system efficiency and fuel stoichiometry vs. power system value.

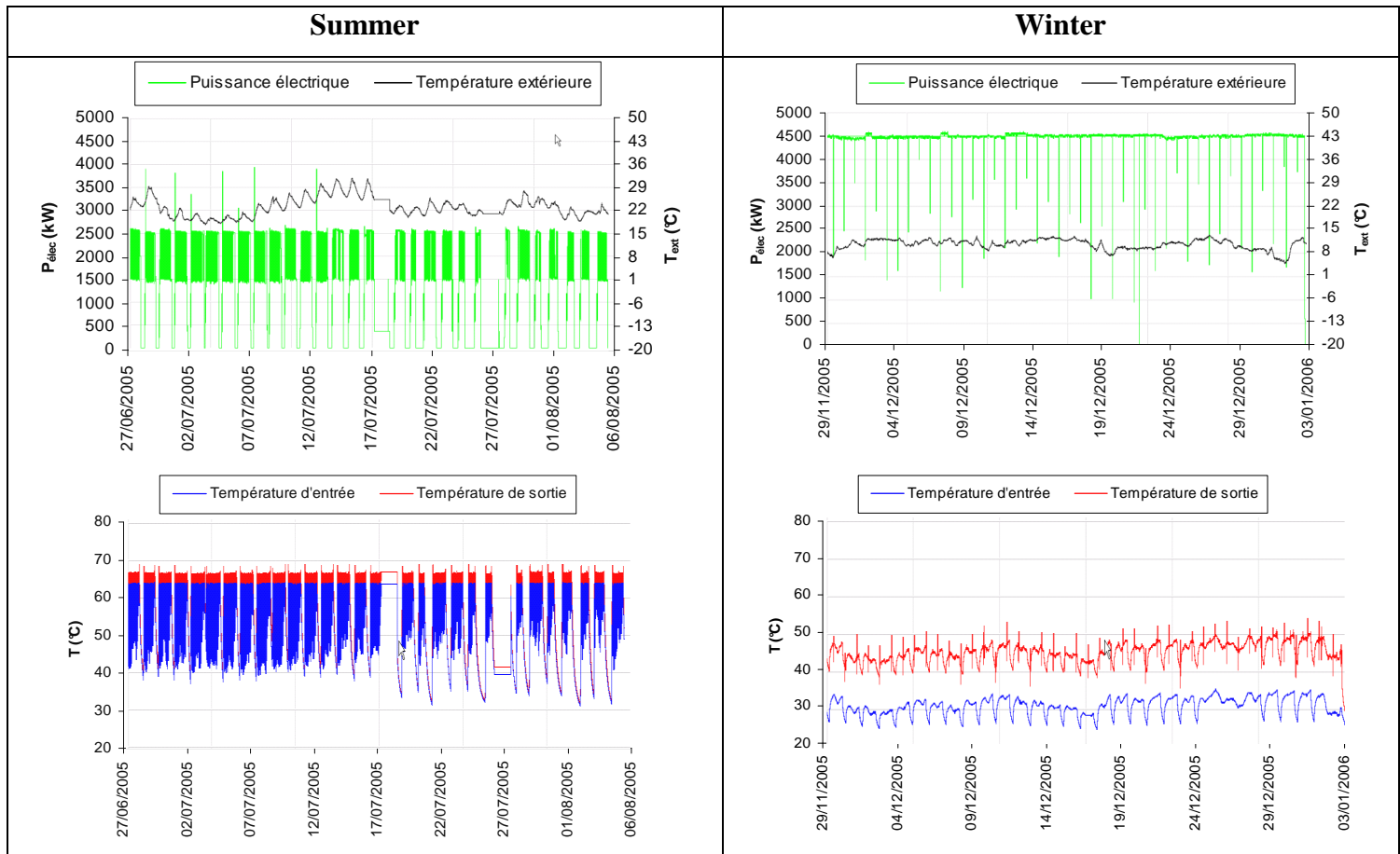


Fig. 21 The figure presents the operation pattern at the Orléans test site during summer (left) and winter (right) periods. The upper two figures display the electric power production (green) and the average outdoor temperature (black). The lower two figures show the stack temperature [inlet: blue and outlet: red]. During winter operation the fuel cell is predominantly operating at full power – 0.4 A/cm<sup>2</sup>, whereas in the summer time the production is stopped almost daily due to insufficient heating demand.

### 2.2.1.3 Other operational parameters

The other important stack operational conditions are listed below:

- Fuel anode stoichiometry:  $\lambda_{H_2} = 1.1^8$  ()
- Air cathode stoichiometry:  $\lambda_{Air} = 2.5$
- Stack<sub>T</sub>: 65°C (cf. Fig. 21-23)
- Max current: 0.4 A/cm<sup>2</sup> (estimated)
- Pressure: 1.02 (abs)
- Min flow of reactants: NA
- Reactant dew point: NA

<sup>8</sup> Range  $\lambda_{H_2}$ . 1.1-1.8 according to the operating conditions -see Lab testing results below

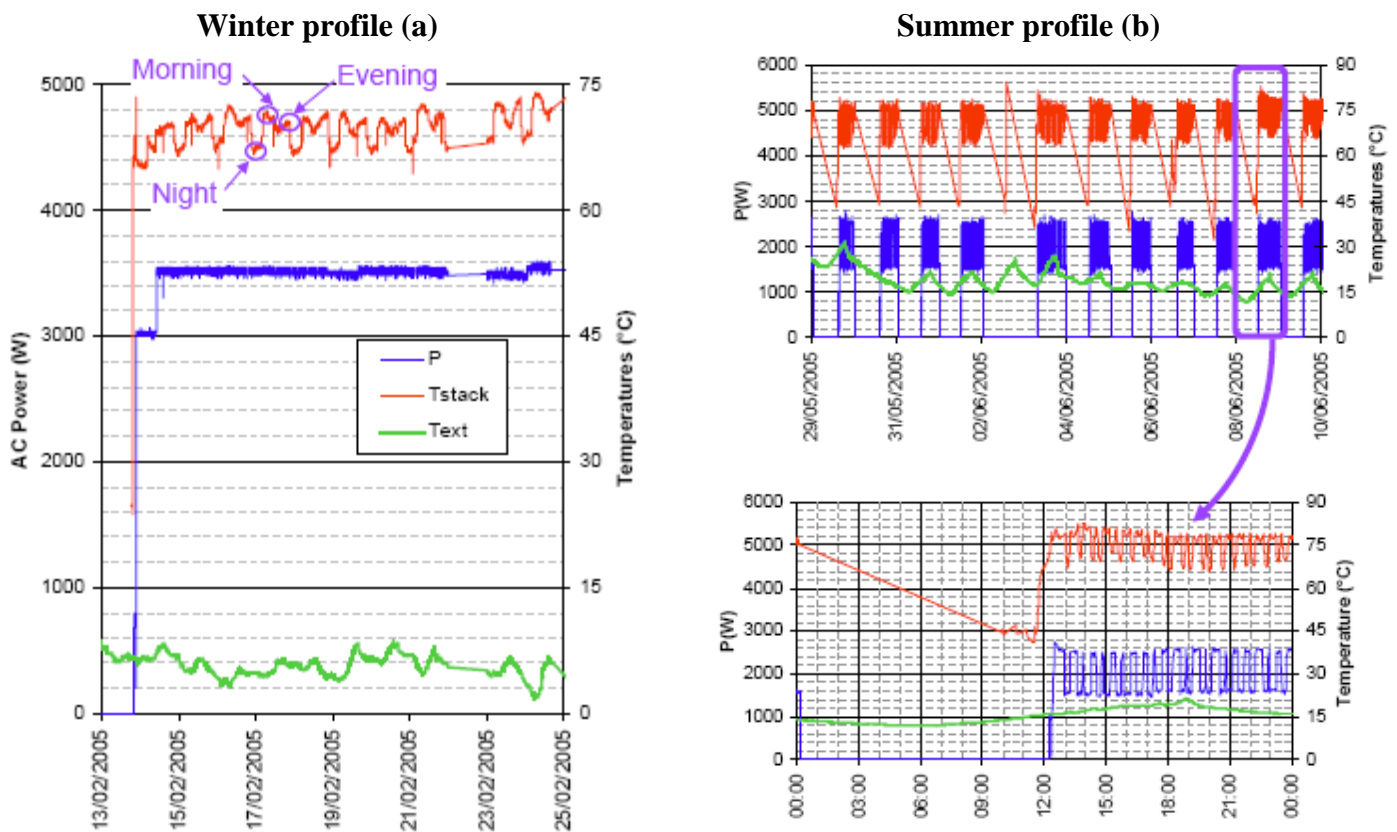


Fig. 22 Influence of seasons on AC-power production and the corresponding stack temperature (exhaust temperature).

Finally, the current supplied by the stack is delivered on the electrical network under a modophasic mode (230 V<sub>AC</sub>, 50 Hz) and after the DC/AC converter step.

#### 2.2.1.4 Start-up

The system starts with a purge of the enclosure with air ( $\approx 12$  min), which ensures the absence of combustible gases in the system. Then the reformer gets purged with natural gas, to avoid local hotspots, which could possibly damage the reformer. After that, the reformer starts heating up ( $\approx 20$  min), first electrically and then using NG. From this point, the production of thermal power usually already starts (30 min after starting the system). After 2.25 hours the reformer is ready for operation, the system switches on the gas supply of the stack.

The duration of the cold start-up is  $\approx 2.5$  h, of warm start-up 2 h until the system is a full electric power output.

#### 2.2.2 PERFORMANCE

The system is in operation for two years without any major failures. The system consumed in this period 16,339 m<sup>3</sup> of natural gas and produced 39,195 kWh of electricity and 103,228 kWh of heat. Electrical and thermal efficiencies reached 23.3 % and 61.5% respectively, resulting in a total efficiency of 84.6 %. These values show that the system performs less efficient than claimed by the company, in particular the electrical production which was claimed to reach 30% is considerably lower than expected, see table 1. This is possibly due to a higher content of periods where the fuel

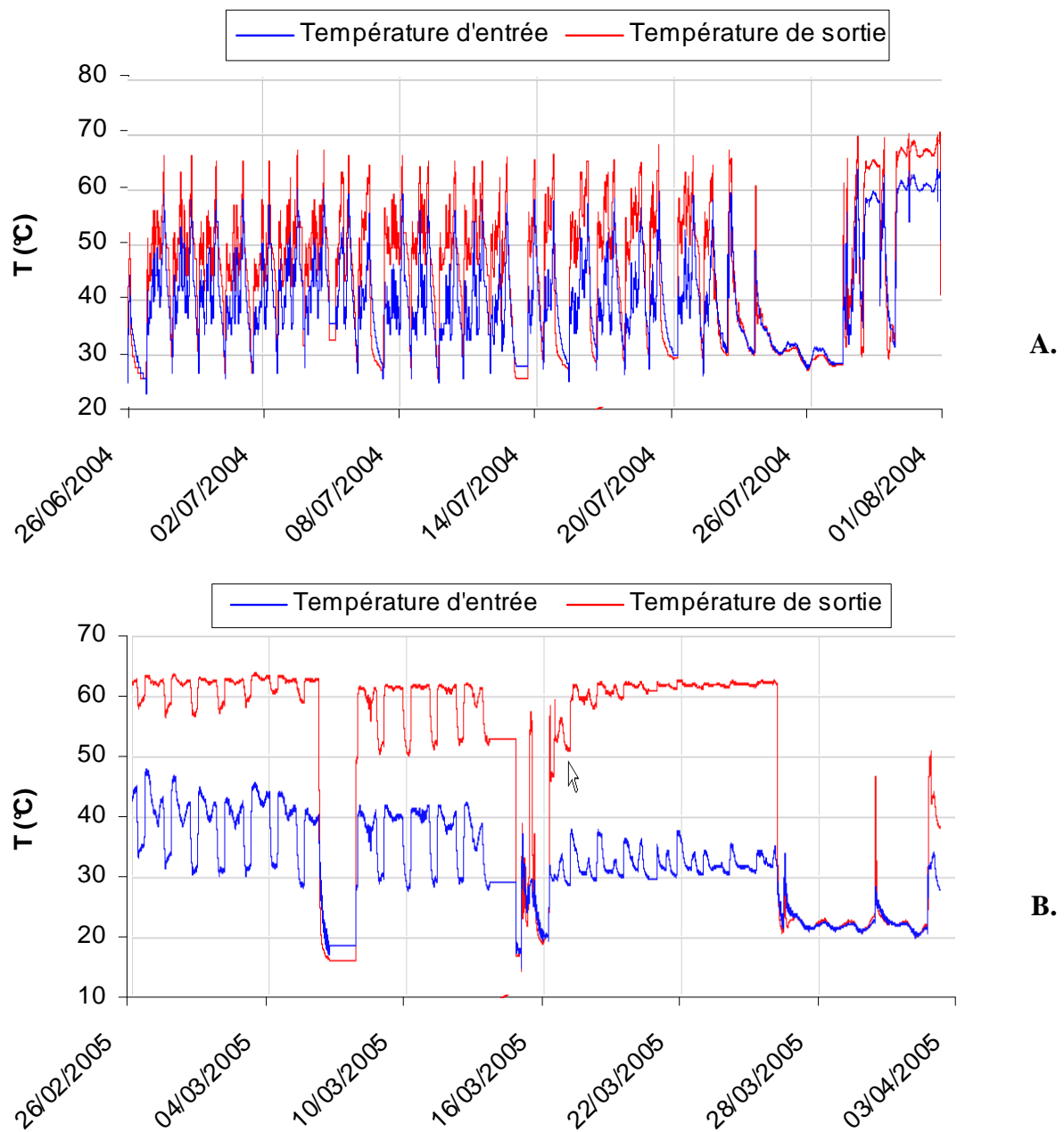


Fig. 23 Typical seasonal LT PEM stack temperature [blue: inlet & Red: outlet] at the Sarreguemines field test site during summer [A] and winter [B].

cell is not operated at maximum power. In particular operation during warm periods, where the system is not running on highest power set point, a decrease in the electrical efficiency is observed.

The overall efficiency increase with a decrease of electrical efficiency and an increase of thermal efficiency when the output AC electrical power on Euro2 system is increased (Fig. 20). This is caused by a higher excess of  $H_2$ , which gets burnt by the reformer, and thereby leads to higher thermal power output and a lower electrical efficiency.

Fig. 21-23 display examples of the operating conditions during summer and winter respectively. In the summer period the outdoor temperature is relatively high and the heating demand is therefore relatively low. This is also seen from the small difference in inlet and outlet temperatures of the



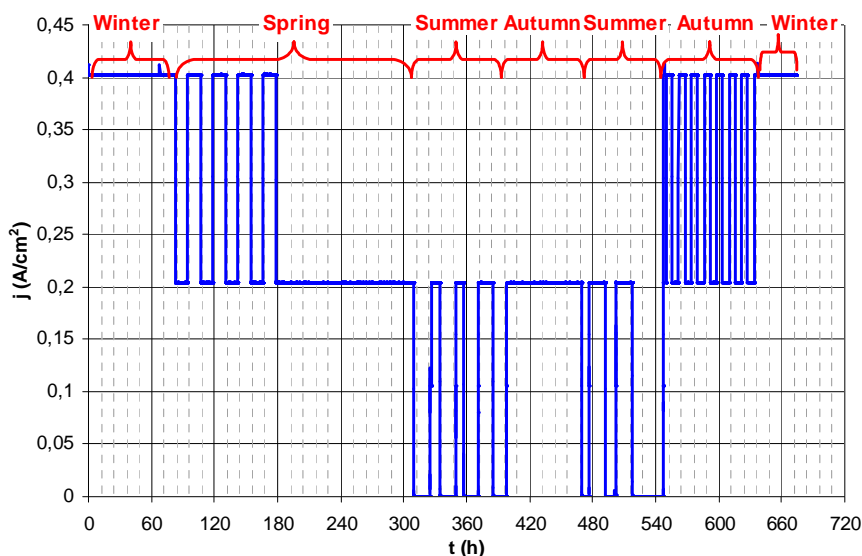


Fig. 24

Current profile for simulating field operation test. The profile describes the power demand corresponding to each season.

cooling water. In this period the fuel cell is altering between stand by and a low power set point. The fuel cell is almost switched off once a day in this period generating a high number of start stop cycles. In the winter period the situation is very different. Here the heating demand is considerably higher, seen from the lower stack temperature [efficient heat exchange] and the high difference in inlet and outlet water temperature. The fuel cell is at maximum power in the majority of the operation time in this period which results in a significantly higher electrical power conversion efficiency.

From the field test a typical power demand profile have been extracted, see Fig. 24. This may then be adopted in laboratory experiments.

Fig. 25 describes the monthly evolution of total energy produced (thermal and electrical) by the LT-PEM FC stack during the whole period of field test. It is observed several months where the energy production is highly below the average. The total efficiency of the system is between 63 and 96% (11 to 34% for electrical efficiency). A wide variation of values is noticed. This fact is mainly induced by the shut down events history of the system (insufficient thermal demand during summer period, maintenance interval, operation of the system in degraded mode due to malfunction or technical faults of the system).

### 2.2.3 RELIABILITY OF THE SYSTEM

Availability level of whole test: around 60% in average of operation (70-75% of availability) for a total energy production of around 100 MWh as thermal energy and 22-44 MWh of electrical energy according to the sites considered (Fig. 26).

During operation a range of technical issues were encountered. This resulted in a range of events where the system needed to be stopped for maintenance. Two indicators were defined in order to characterise the availability:

- The operation time: The ratio between the operation time and the total time period
- The available time: The ratio between the time the system is available and the total time period

Over the complete test period the operation time was 63.2% and the available time were 75.4%

The operation time and available time is presented for each month of the entire test period in Fig. 27. After the first year it was decided to shut down the system during some of the summer months in order to prevent the undesired start/stop cycles which typically is necessary in the summer, see Fig. 21. The sources of break down are summarised in Fig. 28 & 29. It is seen that the main issue is the system auxiliary periods (42%).

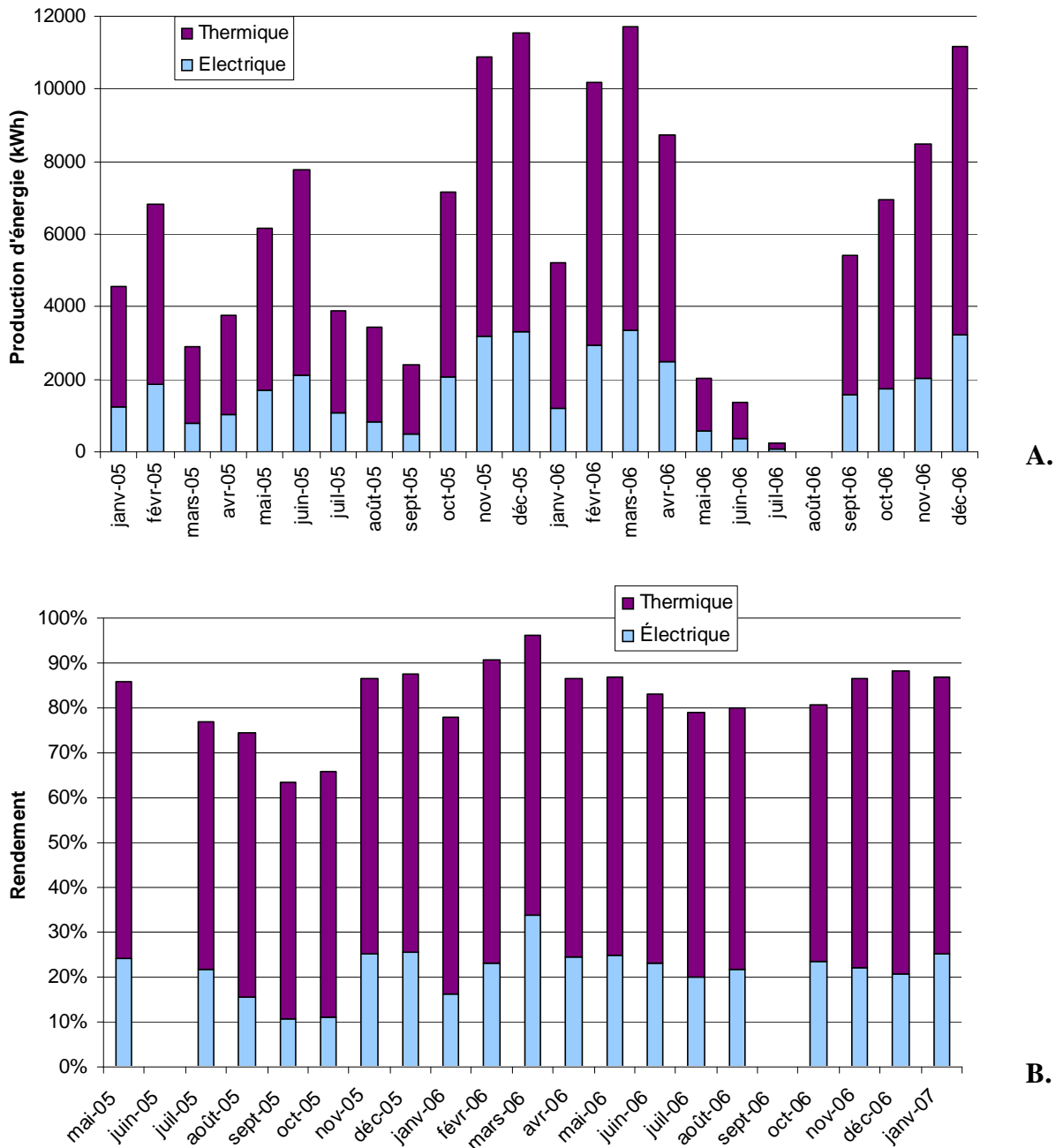


Fig. 25 Evolution of electrical and thermal monthly energy (A) and the corresponding efficiencies (B) produced by Vaillant system.

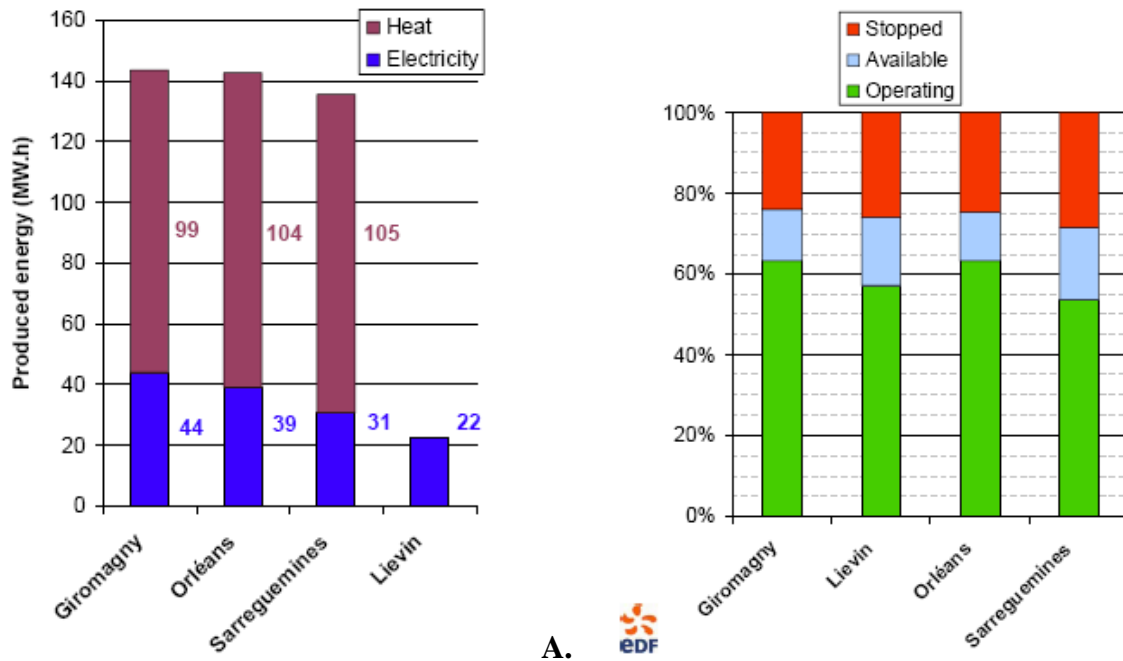


Fig. 26 Evolution of electrical and thermal monthly energy (A) and the corresponding efficiencies (B) produced by Vaillant system.

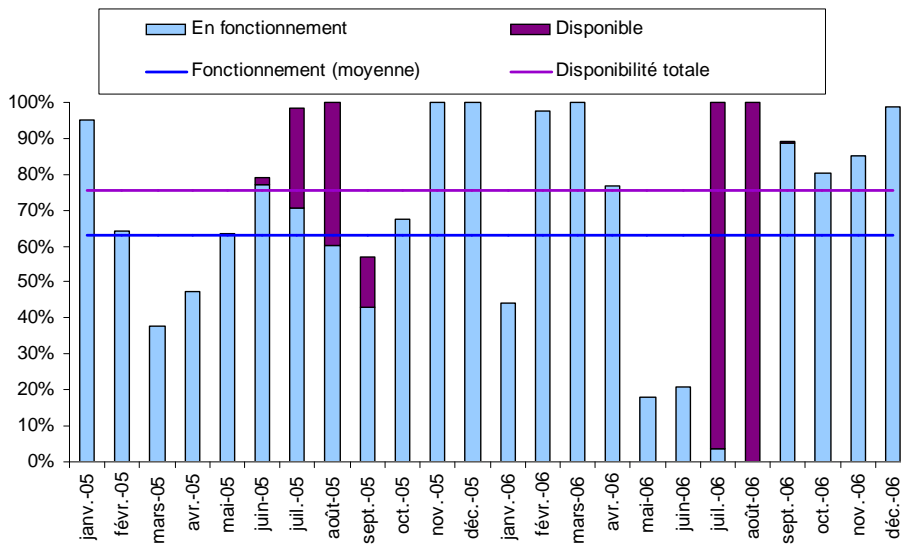


Fig. 27 Overview of operation time and available time of each month of the test period. In most of July and August 2006 the system was switched off in order to avoid start stop cycling of the system.

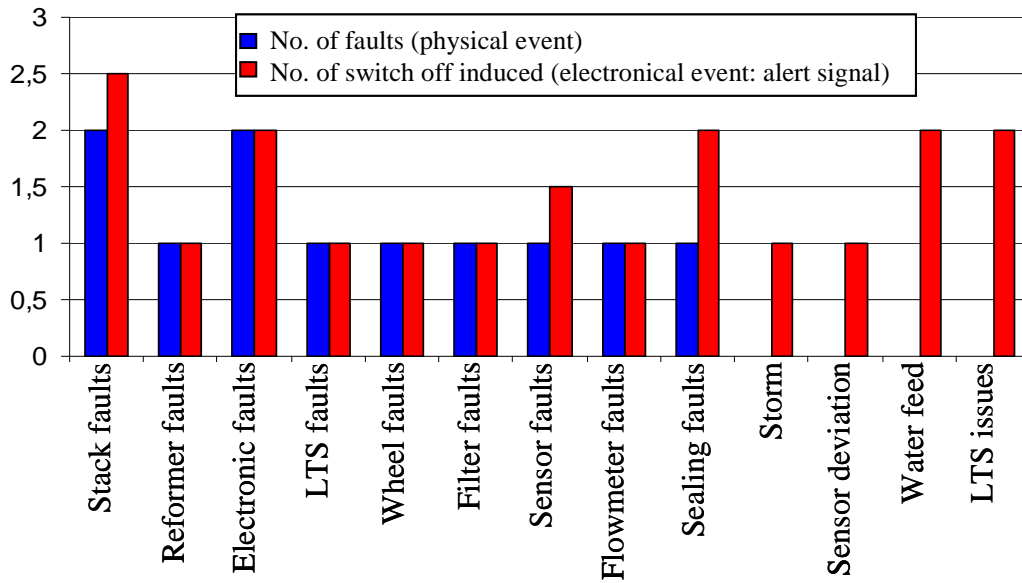


Fig. 28

Maintenance events realized on Vaillant Fuel Cell during the test. Some alert signals have been induced by two parts of the system (in particular stacks alert + methan sensor alert).

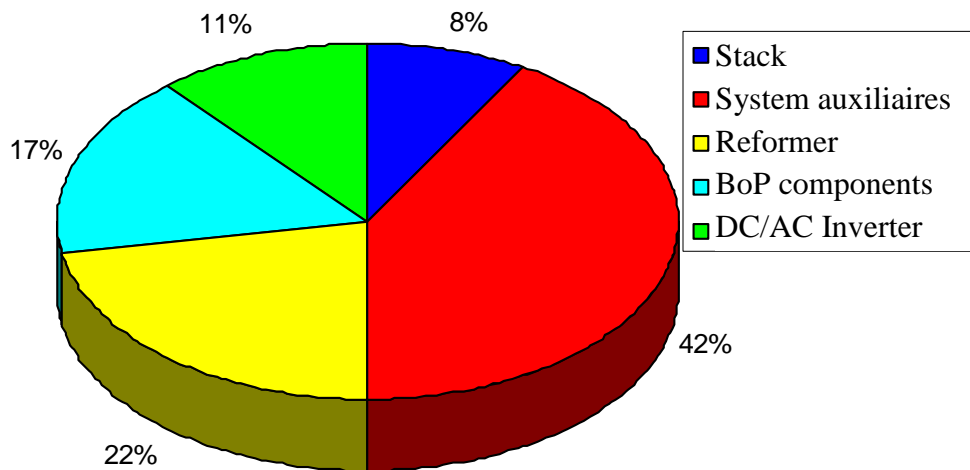
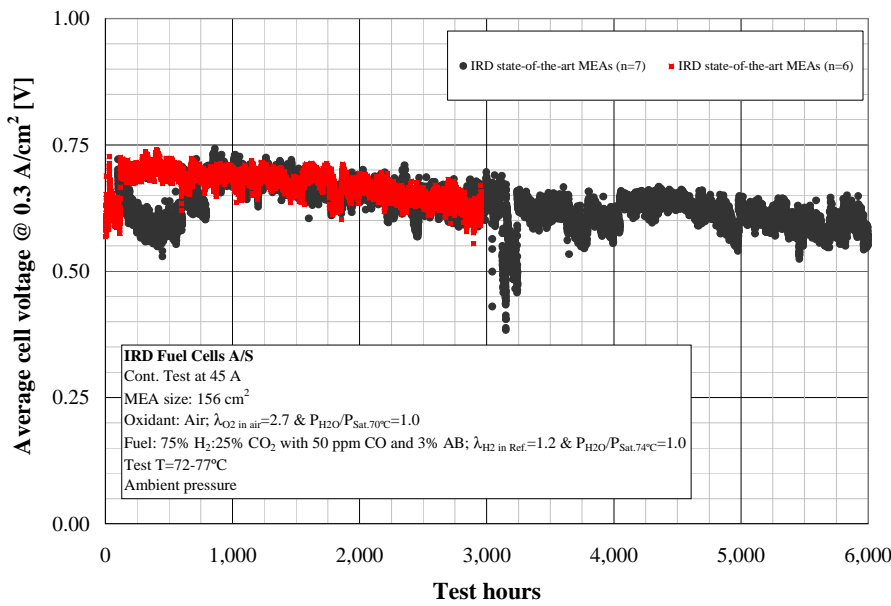


Fig. 29 Overview of system failure modes during the 20-month long field test. System auxiliaries includes LTS fault, seal faults etc.

The Vaillant field test consisted of assessing the reliability and performance of a complete LT PEM FC commercial system connected to the EDF customers energy demand of a collective residential site. The stack (and so MEAs inside) has not been exchanged during the whole period.

### 2.3 LT PEM FC MEA OPERATION WITH SIMULATED REFORMAT

A long-term MEA test in an open-end fuel configuration has been performed at IRD (Fig. 30). The test indicate that reinforcing the MEAs may be very attractive i.e. a constant voltage degradation of 2  $\mu$ V/h will result in a lifetime of plus 20,000 hours, if the EoL definition is a 10% voltage loss.



A.

Fig. 30

Long-term MEA test in simulated reformat containing 75% H<sub>2</sub>; 25% CO<sub>2</sub>; 50 ppm CO & 3% air bleed. The other relevant operational test conditions are as follows:

$\lambda_{H_2}$ : 1.2

Fuel dew point: 74°C

$\lambda_{O_2}$ : 2.7

Air dew point: 70°C

T-in: 72°C

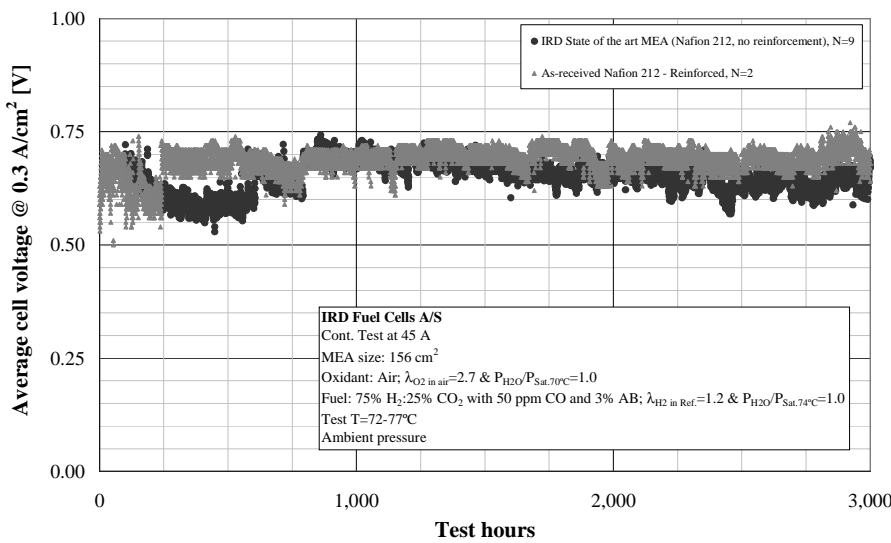
T-out: 77°C

A. State-of-the-art IRD MEAs.

Measured degradation rate is 10  $\mu$ V/h. The MEAs has been exposed to more than 1,200 start/stop cycles

B. Reinforced MEAs in comparison with state-of-the-art MEAs (A).

The measured degradation rate is <2  $\mu$ V/h. The MEAs has been exposed to more than 300 start/stop cycles



B.

### 3 CONCLUSION AND RECOMMENDATIONS

---

It is obvious that the main failure mechanism that has been observed in both reported field tests is malfunctioning or badly controlled BoP and control. All these failures have resulted in LT PEM FC degradations and often in reel MEA ‘destructions’. The scope of this project is to enhance the LT PEM durability and lifetime. Part of this ought to be related to the BoP/control and part of this is related to enhancing the robustness of the LT PEM MEA and stack. An expected important outcome of this project is improved understanding of the optimal operational conditions. This will be gained through the extensive tests planned. The experience obtained in the two field tests reported has pin-pointed the following topics that are essential to enhance the LT PEM durability and lifetime:

1. Improve the MEA and in particular the membrane with respect to mechanical properties i.e. to withstand the pressure pulses at the dead-end operation
2. Improve the catalyst support durability in order to minimise the possibility of carbon corrosion in case of fuel starvation e.g. flooding
3. Improve the long-time water management of the electrodes and the GDL
4. Improve the long-time hydrophobicity of the bipolar plate flow channels
5. Define optimised start and stop procedures
6. Develop operational strategies for dead-end dry hydrogen operation

It is furthermore recommended to improve the membrane and catalyst tolerance towards fuel impurities as a commercial  $\mu$ CHP product is not likely to be equipped with expensive filters. It is recommended to improve the MEA tolerance towards ammonia, NOX, soot, salt and other pollutant that may occur in uncontrolled amount.



## 4 REFERENCES

---

- P. Mocoteguy, B. Ludwig, J. Scholta, R. Barrera, and S. Ginocchio, Long Term Testing in Continuous Mode of HT-PEMFC Based H<sub>3</sub>PO<sub>4</sub>/PBI Celtec-P MEAs for  $\mu$ -CHP Applications, *Fuel Cells (Weinheim, Ger.)*, **9**, 325-348 (2009)
- P. Mocoteguy, B. Ludwig, J. Scholta, Y. Nedellec, D. J. Jones, and J. Roziere, Long-Term Testing in Dynamic Mode of HT-PEMFC H<sub>3</sub>PO<sub>4</sub>/PBI Celtec-P Based Membrane Electrode Assemblies for Micro-CHP Applications, *Fuel Cells (Weinheim, Ger.)*, **10**, 299-311 (2010)
- S. Motupally (2007): Degradation Mechanisms in Transportation PEM Fuel Cells. UTC Power presentation at «The international Workshop on degradation issues of Fuel Cells», 19-21 Sep. 2007, Crete, Greece

## ANNEX 1. ABBREVIATIONS

---

AST	<u>A</u> ccelerated <u>S</u> tress <u>T</u> est
ATR	<u>A</u> uto <u>T</u> hermal <u>R</u> eaction
BoL	<u>B</u> eginning- <u>o</u> f- <u>L</u> ife
BoP	<u>B</u> alance- <u>o</u> f- <u>P</u> lant
CCB	<u>C</u> atalyst <u>C</u> oated <u>B</u> acking
CCM	<u>C</u> atalyst- <u>C</u> oated <u>M</u> embrane
CVMS	<u>C</u> ell <u>V</u> oltage <u>M</u> onitoring <u>S</u> ystem
DGC	The Danish Gas Technological Centre (Danish: <u>D</u> ansk <u>G</u> asteknologisk <u>C</u> enter)
EoL	<u>E</u> nd- <u>o</u> f- <u>L</u> ife
FC	<u>F</u> uel <u>C</u> ell
GDL	<u>G</u> as <u>D</u> iffusion <u>L</u> ayer
LT	<u>L</u> ow <u>T</u> emperature
LTS	<u>L</u> ow <u>T</u> emperature gas <u>S</u> hift
MEA	<u>M</u> embrane <u>E</u> lectrode <u>A</u> ssemblies
OCV	<u>O</u> pen <u>C</u> ell <u>V</u> oltage
PEM	<u>P</u> roton <u>E</u> xchangeable <u>M</u> embrane
VPP	<u>V</u> irtual <u>P</u> ower <u>P</u> lant